

1     **Temporal Stability and Molecular Persistence of the Bone Marrow Plasma**  
2                                     **Cell Antibody Repertoire**

3  
4             Gabriel C. Wu<sup>1</sup>, Nai-Kong V. Cheung<sup>3</sup>, George Georgiou<sup>2,4,5,6</sup>, Edward M.  
5                             Marcotte<sup>1,2,6\*</sup> and Gregory C. Ippolito<sup>2,\*</sup>

- 6  
7     1.     Center for Systems and Synthetic Biology University of Texas at Austin,  
8             Austin, TX, USA  
9     2.     Department of Molecular Biosciences, University of Texas at Austin, Austin,  
10            Texas, USA  
11    3.     Department of Pediatrics, Memorial Sloan-Kettering Cancer Center, New  
12            York, New York, USA  
13    4.     Department of Biomedical Engineering, University of Texas at Austin, Austin,  
14            Texas, USA  
15    5.     Department of Chemical Engineering, University of Texas at Austin, Austin,  
16            Texas, USA  
17    6.     Institute for Cell and Molecular Biology, University of Texas at Austin, Austin,  
18            TX, USA

19  
20  
21  
22  
23    \*To whom correspondence should be addressed: Edward M. Marcotte,  
24    marcotte@icmb.utexas.edu; Gregory C. Ippolito, gci@mail.utexas.edu.

28 **ABSTRACT**

29

30 Plasma cells in human bone marrow (BM PCs) are thought to be intrinsically  
31 long-lived and to be responsible for sustaining lifelong immunity through the constitutive  
32 secretion of antibody—but the underlying basis for this serological memory remains  
33 controversial. Here, we analyzed the molecular persistence of serological immunity by  
34 an examination of BM PC immunoglobulin heavy-chain (IGH) transcripts derived from  
35 serial bone marrow specimens obtained during a span of several years. Using high-  
36 throughput sequence analysis of the same individual for 6.5 years, we show that the BM  
37 PC repertoire is remarkably stable over time. We find that the bias in IGH V, D, and J  
38 individual gene usage and also the combinatorial V–D, V–J, D–J, and V–D–J usage  
39 across time to be nearly static. When compared to a second donor with time points 2  
40 years apart, these overall patterns are preserved, and surprisingly, we find high  
41 correlation of gene usage between the two donors. Lastly, we report the persistence of  
42 numerous BM PC clonal clusters (~2%) identifiable across 6.5 years at all time points  
43 assayed, supporting a model of serological memory based, at least in part, upon intrinsic  
44 longevity of human PCs. We anticipate that this longitudinal study will facilitate the ability  
45 to differentiate between healthy and diseased antibody repertoire states, by serving as a  
46 point of comparison with future deep-sequencing studies involving immune intervention.  
47

## 48 INTRODUCTION

49

50 The human bone marrow (BM) is a specialized immune compartment that is  
51 responsible for both the initial generation of newly-formed B cells and also the  
52 maintenance of terminally differentiated, antibody-secreting plasma cells (PCs). The BM,  
53 and the PCs it harbors, is a major site of antibody production and is the major source of  
54 all classes and subclasses of human immunoglobulins (Ig) detectable in the serum<sup>1,2</sup>. Ig-  
55 secreting BM PCs are generally believed to be “long-lived” and maintained for the  
56 lifespan of the organism<sup>3</sup>. In this regard, it has been well established in longitudinal  
57 serological studies that antiviral serum antibodies can be remarkably stable, with half-  
58 lives ranging from 50 years (e.g. varicella-zoster virus) to 200 years for other viruses  
59 (e.g. measles and mumps); however, in contrast, antibody responses to non-replicating  
60 antigens (e.g. tetanus and diphtheria bacterial toxins) rapidly decay with much shorter  
61 half-lives of only 10-20 years<sup>4</sup>. Not only does this suggest that antigen-specific  
62 mechanisms play a substantial role in the establishment and/or maintenance of  
63 serological memory, but raises the question of whether the differential stability of  
64 antibody responses might reflect differential intrinsic longevity of PCs themselves. This  
65 has been previously proposed in the context of vaccinations and infections<sup>4,5</sup>, and is also  
66 supported by observations of differential stability of autoantibody titers when using B-cell  
67 depleting therapies to treat autoimmune diseases<sup>6,7</sup>.

68 The basis underlying lifelong serological memory (antibody responses) remains  
69 controversial<sup>3,8,9</sup>. Data supporting a model for intrinsic longevity in PC survival (and  
70 hence longevity in serum antibody maintenance) has been posited for the laboratory  
71 mouse<sup>10,11</sup>, but data for human PCs are absent. Based upon the murine models, it has  
72 been assumed that human BM PCs are similarly long-lived and that these long-lived  
73 PCs are the major source of serum antibodies; however, only recently have antigen-  
74 specific BM PCs been ascertained for their contribution to the pool of serum antibodies  
75 in humans<sup>5,12</sup>. Despite these notable advances, the availability of corresponding  
76 molecular data (namely, sequence data of BM PC Ig transcripts) and of information  
77 regarding PC dynamics *in vivo* are scarce.

78 Three studies have generated BM PC data using next-generation sequencing  
79 techniques, but none of which have examined the temporal changes that occur in the  
80 immune repertoire over time<sup>5,13,14</sup>. Here, building upon our prior experiences with the

81 comprehensive analysis of human cellular and serological antibody repertoires<sup>15–19</sup>, we  
82 present the first longitudinal study of serially acquired human BM PCs assayed by next-  
83 generation deep sequencing. To directly measure the temporal dynamics of BM PCs—  
84 and to indirectly gain insight into long-lived serological memory—we sequenced the  
85 recombined VHDJH region, which encodes the variable region (V domain) of IGH heavy  
86 chains of BM PCs from the same individual over seven timepoints encompassing a total  
87 of 6.5 years and from a second individual with two timepoints over 2.3 years. The  
88 temporal resolution and duration of sampling provides a method to interrogate the *in vivo*  
89 temporal dynamics of BM PCs in a previously uncharacterized way. We provide detailed  
90 temporal information on the individual genes (IGH V, D, and J), gene combinations (V-D,  
91 V-J, D-J, V-D-J), and persistent CDR-H3 clonotypes. The second individual provides  
92 support that our observations are not unique. Overall, our results (i) underscore the  
93 temporal stability of the IGH V region repertoire according to multiple metrics (temporally  
94 stable IGH molecular phenotypes), and (ii) provide unequivocal sequence-based  
95 evidence for the persistence of PC cellular clonotypes spanning 6.5 years.

96

## 97 **RESULTS**

98

### 99 **Serial Bone Marrow Biopsies Followed by Next-Generation Sequencing** 100 **Demonstrate Temporal Dynamics of the Immune Repertoire.**

101

102 To investigate the temporal dynamics of the IGH antibody gene repertoire of  
103 bone marrow plasma cells (BM PCs), we sampled, sorted, and performed high-  
104 throughput sequencing (Fig. 1a). Serial bone marrow biopsies were obtained from two  
105 adolescents (10–17 years of age) as part of routine evaluations for non-immuno-  
106 hematological disease. BM PCs were isolated using fluorescence-activated cell sorting  
107 (FACS). BM PCs were obtained by sorting for CD38<sup>++</sup> CD138<sup>+</sup> cells within the  
108 mononuclear light-scatter gate (Fig. 1b). Additionally, the cells were uniformly positive  
109 for the TNF-receptor superfamily member CD27 (Fig. 1b, inset). Importantly, we avoided  
110 gating of the pan-B cell marker CD19 since previous characterizations of human BM  
111 PCs show heterogeneous expression of CD19<sup>20,21</sup>. Therefore, our method captured all  
112 recently described BM PC subpopulations<sup>5,12</sup> with an overall CD19<sup>+/-</sup> CD27<sup>+</sup> CD38<sup>++</sup>

113 CD138<sup>+</sup> phenotype. Subsequently, transcripts were amplified from BM PCs expressing  
114 IgM, IgG, and IgA using RT-PCR followed by high-throughput sequencing.

115 In total, 51,200 BM PC were sorted, which generated 503,415 reads after quality-  
116 threshold filtering (see Methods and Supplementary Table S1). These data were  
117 distributed across seven timepoints spanning 6.5 years (Fig. 1c). A biological replicate, a  
118 second frozen ampule derived from the same bone marrow aspiration, was also  
119 collected from each donor and analyzed. Multiple sampling from the same donor allows  
120 us to accurately identify the active heavy chain genes that compose this donor's  
121 antibody repertoire. Specifically, we identify 38 IGHV genes, 21 IGHD genes, and 6  
122 IGHJ genes (4,788 combinations).

123

#### 124 **IGH V, D, and J Frequency Are Highly Stable Over 6.5 Years.**

125

126 To determine the stability of individual gene usage, we assessed the frequency  
127 of each IGH V, D, and J gene across time (Fig. 2). Surprisingly, we saw stable behavior  
128 of these genes, with the most frequently used genes (e.g. IGHV4-34) showing  
129 consistently high expression while less frequently used genes (e.g. IGHV3-72) showed  
130 consistently low expression. This observation was quantified using the Mann-Kendall  
131 Test, which evaluates trends in time series data. We found that 89% of IGHV genes,  
132 95% of IGHD genes and 100% IGHJ genes showed no statistically significant trends  
133 (Mann-Kendall test,  $p > 0.05$ ), indicating that the IGHV (Fig. 2a), IGHD (Fig. 2b), and  
134 IGHJ (Fig. 2c) genes were time stable.

135 Next, we analyzed population behavior of gene usage. Averaging across all  
136 timepoints, we observed a highly skewed distribution of individual gene frequencies,  
137 consistent with previous single timepoint observations. Only 6 IGHV genes (16%)  
138 accounted for greater than 50% of total IGHV gene usage by frequency (Fig. 2d). IGHD  
139 genes that have previously been shown to have biased usage IGHD2-2, IGHD3-3, and  
140 IGHD3-22<sup>22</sup> together accounted for 33% of total IGHD usage (Fig. 2b). In addition,  
141 known biases in IGHJ usage<sup>23</sup> are recapitulated as IGHJ4, IGHJ6, and IGHJ5 account  
142 for 86% of total IGHJ usage. Furthermore, our analysis demonstrated that IGH V, D, and  
143 J gene usage were not significantly different from a log-normal distribution (Anderson-  
144 Darling,  $H=0$ ,  $p > 0.05$ ).

145

#### 146 **IGH V-D, D-J, V-J, and V-D-J Combinations Are Stable Over Time.**

147

148           Given the temporal stability of individual genes, we hypothesized that differential  
149 intrinsic longevity might be found in gene combinations. Surprisingly, our analysis  
150 suggests that gene combinations, like their individual component genes, are time stable  
151 as well. We found that 92% V-J (Fig. 4), 97% V-D (Supplementary Fig. 1a), 95% D-J  
152 (Supplementary Fig. 1b), and 97% V-D-J (Supplementary Fig. 1c) do not show  
153 significant trends (Mann-Kendall,  $H=0$ ,  $p>0.05$ ).

154           To better understand the nature of gene combinations, we analyzed preferential  
155 gene pairing biases by comparing the expected versus observed frequency of pairwise  
156 gene combinations. The observed frequency of each gene combination was found to be  
157 correlated to its expected frequency (Spearman  $r$ ): V-D (0.74), V-J (0.87), D-J (0.93),  
158 and V-D-J (0.65) (Fig. 5a-d). This high level of correlation and lack of significant outliers  
159 suggests that there is minimal gene pairing linkage and that the gene pairing is a  
160 random process.

161

#### 162 **Persistent Clonotypes Are Stable Over Time.**

163

164           To understand how each of these individual genes and gene combinations  
165 together might indicate the existence of long lived PCs, we analyzed the behavior of the  
166 CDR-H3, the highest resolution possible for a single identifier of an antibody producing  
167 cell. To eliminate errors and ambiguities, we clustered CDR-H3s into clonotypes based  
168 on previously established criteria (see Methods). On average, we found that 16% of  
169 clonotypes are shared between adjacent timepoints (Fig. 6a, top). Interestingly, 23  
170 clonotypes persisted across all timepoints (Fig. 6b). We found that 100% of these  
171 persistent clonotypes were time stable (Fig. 6a, bottom, Mann-Kendall test,  $h=0$ ,  $p>0.05$ )  
172 and 78% (18/23) were of the IgA isotype. In addition, characteristics of the complete  
173 CDR-H3 population, specifically CDR-H3 lengths (Supplementary Fig. 2) and hydrophathy  
174 index (Supplementary Fig. 3), are unchanged over time. The overall total distribution of  
175 CDR-H3 lengths are consistent with previously reported single timepoint values<sup>27</sup>. Also,  
176 higher expressing CDR-H3s tended to be neither hydrophobic nor hydrophilic  
177 (Supplementary Fig. 3) and no significant trends between hydrophobicity and expression  
178 level were found.

179

#### 180 **A Second Donor Corroborates The Observations From The First Donor.**

181

182           To verify our longitudinal observations of stability and random gene choices from  
183 Donor 1, we analyzed a second donor across two years (Fig. 7). We identified 38 IGHV  
184 genes, 22 IGHD genes, and 6 IGHJ genes (5,016 combinations, 6,763 cells, 48,525  
185 reads) (Supplementary Table 1 and Supplementary Fig. 4). Donor 1 and Donor 2 show  
186 highly correlated IGHV gene usage ( $r=0.82$ ). Thus, the trends observed in Donor 1 were  
187 also observed in Donor 2. Specifically, individual IGHV, IGHD, and IGHJ gene usages  
188 were time stable (Supplementary Fig. 4), as were the gene combinations  
189 (Supplementary Fig. 5). Consistent with Donor 1, Donor 2 showed no preferential  
190 pairing in gene combinations (Supplementary Fig. 6). These results are highly consistent  
191 with the trends observed in Donor 1, and together, they indicate that BM PC antibody  
192 gene and gene combination usage show surprisingly minimal variation between  
193 individuals and across time.

194

## 195 **DISCUSSION**

196

197           Next-generation sequencing has enabled unprecedented ability to explore the  
198 details of the human immune repertoire<sup>28,29</sup>. Whereas previous studies have been able  
199 to describe some aspects of immune repertoire at a single point in time, our results  
200 harness the power of next-generation sequencing to elucidate the temporal dynamics of  
201 BM PCs over 6.5 years. Importantly, our data provide molecular resolution of antibody  
202 identity in the form of clonotypes, which is not possible with classic techniques like  
203 enzyme-linked immunosorbent assay (ELISA).

204

205           In this study, we show that the immune system is naturally polarized in both gene  
206 choice and gene combination usage and that the polarization is maintained over time.  
207 We also found that the bias is not primarily a result of gene linkage, suggesting there are  
208 additional genomic or extrinsic factors that contribute to polarization. For example, there  
209 may be an E $\mu$  like enhancer in humans that results in higher than expected IGHJ4  
210 usage<sup>30</sup>. Alternatively, the long arms race between the human immune system and the  
211 antigens it faces throughout evolutionary history may have established a preferential  
212 gene choice long ago. So higher expressing genes are likely broad-spectrum antibodies  
213 that have been useful in fighting particular classes of disease and continue to do so

214 today. For example, IGHV1-69 is implicated in many viral diseases like influenza and  
215 HIV. IGHV4-34 is associated with a range of autoimmune disorders, like cold agglutinin  
216 disease and systemic lupus erythematosus (SLE).

217 Taken together, our results indicate that the BM PC antibody gene and gene  
218 combination usage is highly stable over long periods of time. While short term studies  
219 over days, weeks or at most a year show that antigen stimulus can result in dramatic  
220 immune repertoire changes over weeks<sup>31</sup> our study extends over half a decade and is  
221 the longest longitudinal study to date. Given the known resistance we have for a large  
222 and diverse array of pathogenic antigens, it is surprising that the overall effect of these  
223 changes is not reflected in gene usage. This suggests that (i) either the existing immune  
224 gene combinations are established early on or that the mechanism of gene choice  
225 results in consistent bias over long periods of time, (ii) the effective size and variability of  
226 the immune repertoire is restricted, and (iii) antigen challenges in the form of  
227 vaccinations and illness do not have lasting changes at the gene usage level. Therefore,  
228 the immune repertoire must defend against a wide array of pathogens with only relatively  
229 small changes in immune diversity. On the other hand, intrinsic immunological memory  
230 is a well-established concept and BM PCs are thought to persist for long periods of time.  
231 An outstanding question remains of how intrinsic longevity is established and  
232 maintained. Although our results are unable to verify that any particular PC member  
233 persists, we can conclude that the clonotype, which defines binding specificity at the  
234 molecular level, does persist for at least 6.5 years. Our results suggest clonotype  
235 persistence contributes to the mechanism underlying long term immunological memory.

236 Moreover, we observe steady usage of gene and gene combinations throughout  
237 our experiment. Our observations suggest that there are large resident pools of plasma  
238 cells of the same identity, from which we can sample continuously with no loss of relative  
239 expression levels. We conclude that a large population of clonally-related PCs is  
240 responsible for persistent and stable gene expression of a given antibody, and that any  
241 given PC clone does not contribute greatly to the overall expression of that antibody.

242 In conclusion, we have used high-throughput, next-generation sequencing to  
243 definitively identify long-term persistent BM PC clonotypes, which has implications in  
244 clinical intervention studies, vaccines, and immunotherapy. Future next-generation  
245 sequencing studies can provide an even more detailed picture of the B cell immune  
246 repertoire as these studies could include advances in VH:VL native-pair sequencing  
247 (paired BCR-seq<sup>19</sup>), the analysis of correlations between BM PC repertoires and serum



248 immunoglobulin species (Ig-seq<sup>17,18</sup>), and an examination of the connectivity of B cells at  
249 various developmental stages (e.g., clonal relationships between circulating memory B  
250 cells and sessile BM PCs) . Our study provides a foundation upon which these further  
251 studies can be built.

252

## 253 **MATERIALS & METHODS**

254

### 255 **Bone Marrow Specimens**

256

257 Serially acquired human bone marrow specimens were collected from two donors by  
258 aspiration from the iliac crest, and mononuclear cells were enriched by Ficoll hypaque  
259 centrifugation. The two adolescent–teenage donors were originally diagnosed with  
260 neuroblastoma but had been asymptomatic and disease-free for many years according  
261 to routine bone marrow histology. A complete description of the donors' past medical  
262 history and ages at the time of the multiple time point collections is included in  
263 Supplementary Table 1. All procedures were performed per a standard operating  
264 procedure at the Memorial Sloan-Kettering Cancer Center and collected according to a  
265 longstanding protocol approved by the MSKCC Institutional Review Board. Aspirates  
266 were withdrawn from four sites and combined (total of 8–10 mL from 4 sites, 2–2.5 mL  
267 per site) drawn from the following: anterior right iliac crest, anterior left iliac crest,  
268 posterior right iliac crest, and posterior left iliac crest. The same attending physicians  
269 performed these procedures and usually biopsied through the same surgical site each  
270 time. De-identified specimens were shipped overnight on dry ice to the University of  
271 Texas at Austin.

272

### 273 **Flow Cytometry and Isolation of Plasma Cells (PC)**

274

275 BM samples were quick-thawed in a 37 °C H<sub>2</sub>O bath and slowly diluted into RPMI-1640  
276 complete medium containing DNaseI (Sigma D 4513; 20 U/mL), pelleted, washed and  
277 re-suspended in 2 mL FACS buffer (Dulbecco's PBS + 0.5% BSA Fraction V). Cell  
278 viability was determined using Trypan Blue exclusion and on average was approximately  
279 90% per specimen. After a one-hour recovery at room temperature, BM cells were  
280 stained for 30 minutes at room temperature using empirically-determined optimal  
281 titrations of monoclonal antibodies: CD38-FITC (HIT2), CD138-PE (B-B4), CD27-APC

282 (M-T271), and CD19-v450 (HIB19). CD19<sup>+</sup>-CD38<sup>++</sup>CD138<sup>+</sup> cells in human BM were  
283 collected as plasma cells (PC). PCs were observed to be heterogeneous for expression  
284 of the CD19 B-lineage marker; therefore, CD19-gating was avoided. CD38<sup>++</sup>CD138<sup>+</sup>  
285 PCs were additionally gated by light scatter properties (FSC v. SSC) to exclude debris,  
286 apoptotic cells, and remnant granulocytes. All cell sorts were performed on a FACSAria  
287 flow cytometer. Cells were sorted directly into TRI Reagent for RNA preservation.

288

### 289 **RT-PCR, High Throughput Sequencing of IGH V, D, and J Genes**

290

291 All methods and reagents were as previously described<sup>15</sup>. Variable genes (recombined  
292 VHDJH region, which encodes the V domain) of IGH isotypes IgM, IgG, and IgA were  
293 amplified from oligo-dT cDNA and sequenced at high-throughput using the Roche 454  
294 GS FLX technology using titanium long-read chemistry.

295

### 296 **Data Processing, Analysis, and Visualization**

297

298 All sequence data have been deposited to NCBI SRA under BioProject number  
299 PRJNA310043. IGHV, IGHD, IGHJ, and CDR-H3 regions for each read was quality  
300 filtered, processed and annotated using the VDJFasta utility described previously<sup>32</sup>.  
301 Reference IGHV, IGHD, and IGHJ genes from the international ImMunoGeneTics  
302 (IMGT) database were used. Mann-Kendall Tests were performed in Matlab, against the  
303 null hypothesis of no trend (alpha=0.05). Spearman r non-parametric correlation analysis  
304 was performed in python using the scipy library. To perform clonal clustering analysis,  
305 CDR-H3 sequences were clustered to form clonotypes, as established previously<sup>33,34</sup>,  
306 using CD-HIT<sup>35</sup> with the following criteria: (i) Same IGHV and IGHJ, (ii) minimum length  
307 of 5, and (iii) 85% similarity threshold on the amino acid level.

308

309 Circular visualization plots were created with Circos software v0.67-7<sup>36</sup> where genes  
310 were sorted by expression within each timepoint and connected to adjacent timepoints  
311 via colored lines showing their expression levels. All other data visualization was  
312 performed using Python and matplotlib.

313

### 314 **Acknowledgements**

315

316 This work was supported by NSF Graduate Research Fellowship DGE-1110007 (to  
317 GCW), HDTRA1-12-C-0105 from DTRA (GG, GCI, EMM), and grants from the NIH,  
318 NSF, and Welch Foundation (F-1515) to EMM.

319

320 **Authorship contributions**

321

322 GG and NKC conceived the study. GCW and GCI designed and performed experiments,  
323 analyzed data, prepared figures, and wrote the manuscript, under the supervision of  
324 EMM. All authors reviewed the manuscript.

325

326 **Conflict of Interest**

327

328 The authors declare no conflict of interest.

329

330

331 **REFERENCES**

- 332 1. McMillan, R. *et al.* Immunoglobulin synthesis by human lymphoid tissues: normal  
333 bone marrow as a major site of IgG production. *J. Immunol.* **109**, 1386–94 (1972).
- 334 2. Benner, R., Hijmans, W. & Haaijman, J. J. The bone marrow: the major source of  
335 serum immunoglobulins, but still a neglected site of antibody formation. *Clin. Exp.*  
336 *Immunol.* **46**, 1–8 (1981).
- 337 3. Radbruch, A. *et al.* Competence and competition: the challenge of becoming a  
338 long-lived plasma cell. *Nat. Rev. Immunol.* **6**, 741–50 (2006).
- 339 4. Amanna, I. J., Carlson, N. E. & Slifka, M. K. Duration of humoral immunity to  
340 common viral and vaccine antigens. *N. Engl. J. Med.* **357**, 1903–15 (2007).
- 341 5. Halliley, J. L. *et al.* Long-Lived Plasma Cells Are Contained within the  
342 CD19–CD38hiCD138+ Subset in Human Bone Marrow. *Immunity* **43**, 132–45  
343 (2015).
- 344 6. Cambridge, G. *et al.* Serologic changes following B lymphocyte depletion therapy  
345 for rheumatoid arthritis. *Arthritis Rheum.* **48**, 2146–54 (2003).
- 346 7. Cambridge, G. *et al.* B cell depletion therapy in systemic lupus erythematosus:  
347 effect on autoantibody and antimicrobial antibody profiles. *Arthritis Rheum.* **54**,  
348 3612–22 (2006).
- 349 8. Amanna, I. J. & Slifka, M. K. Contributions of humoral and cellular immunity to  
350 vaccine-induced protection in humans. *Virology* **411**, 206–15 (2011).
- 351 9. Zinkernagel, R. On plasma cell longevity or brevity. *Expert Rev. Vaccines* **13**,  
352 821–3 (2014).
- 353 10. Manz, R. A., Thiel, A. & Radbruch, A. Lifetime of plasma cells in the bone marrow.  
354 *Nature* **388**, 133–4 (1997).
- 355 11. Slifka, M. K., Antia, R., Whitmire, J. K. & Ahmed, R. Humoral immunity due to  
356 long-lived plasma cells. *Immunity* **8**, 363–72 (1998).
- 357 12. Mei, H. E. *et al.* A unique population of IgG-expressing plasma cells lacking CD19  
358 is enriched in human bone marrow. *Blood* **125**, 1739–48 (2015).
- 359 13. Cowan, G. *et al.* Massive parallel IGHV gene sequencing reveals a germinal  
360 center pathway in origins of human multiple myeloma. *Oncotarget* **6**, 13229–40  
361 (2015).
- 362 14. Tschumper, R. C. *et al.* Comprehensive assessment of potential multiple  
363 myeloma immunoglobulin heavy chain V-D-J intraclonal variation using massively  
364 parallel pyrosequencing. *Oncotarget* **3**, 502–13 (2012).

- 365 15. Ippolito, G. C. *et al.* Antibody repertoires in humanized NOD-scid-IL2R $\gamma$ (null) mice  
366 and human B cells reveals human-like diversification and tolerance checkpoints in  
367 the mouse. *PLoS One* **7**, e35497 (2012).
- 368 16. DeKosky, B. J. *et al.* High-throughput sequencing of the paired human  
369 immunoglobulin heavy and light chain repertoire. *Nat. Biotechnol.* **31**, 166–9  
370 (2013).
- 371 17. Wine, Y. *et al.* Molecular deconvolution of the monoclonal antibodies that  
372 comprise the polyclonal serum response. *Proc. Natl. Acad. Sci. U. S. A.* **110**,  
373 2993–8 (2013).
- 374 18. Lavinder, J. J. *et al.* Identification and characterization of the constituent human  
375 serum antibodies elicited by vaccination. *Proc. Natl. Acad. Sci. U. S. A.* **111**,  
376 2259–64 (2014).
- 377 19. DeKosky, B. J. *et al.* In-depth determination and analysis of the human paired  
378 heavy- and light-chain antibody repertoire. *Nat. Med.* **21**, 86–91 (2014).
- 379 20. Kaminski, D. A., Wei, C., Qian, Y., Rosenberg, A. F. & Sanz, I. Advances in  
380 Human B Cell Phenotypic Profiling. *Front. Immunol.* **3**, 302 (2012).
- 381 21. Flores-Montero, J. *et al.* Immunophenotype of normal vs. myeloma plasma cells:  
382 Toward antibody panel specifications for MRD detection in multiple myeloma.  
383 *Cytometry B. Clin. Cytom.* (2015). doi:10.1002/cyto.b.21265
- 384 22. Larimore, K., McCormick, M. W., Robins, H. S. & Greenberg, P. D. Shaping of  
385 human germline IgH repertoires revealed by deep sequencing. *J. Immunol.* **189**,  
386 3221–30 (2012).
- 387 23. Wasserman, R. *et al.* The pattern of joining (JH) gene usage in the human IgH  
388 chain is established predominantly at the B precursor cell stage. *J. Immunol.* **149**,  
389 511–6 (1992).
- 390 24. Theofilopoulos, A. N. & Bona, A. N. *The Molecular Pathology of Autoimmune*  
391 *Diseases*. (CRC Press, 2002).
- 392 25. Mortuza, F. Y. Immunoglobulin heavy-chain gene rearrangement in adult acute  
393 lymphoblastic leukemia reveals preferential usage of JH-proximal variable gene  
394 segments. *Blood* **97**, 2716–2726 (2001).
- 395 26. Berman, J. E. *et al.* VH gene usage in humans: biased usage of the VH6 gene in  
396 immature B lymphoid cells. *Eur. J. Immunol.* **21**, 1311–4 (1991).
- 397 27. Rao, S. P. *et al.* Biased VH gene usage in early lineage human B cells: evidence  
398 for preferential Ig gene rearrangement in the absence of selection. *J. Immunol.*  
399 **163**, 2732–40 (1999).

- 400 28. Georgiou, G. *et al.* The promise and challenge of high-throughput sequencing of  
401 the antibody repertoire. *Nat. Biotechnol.* **32**, 158–68 (2014).
- 402 29. Wine, Y., Horton, A. P., Ippolito, G. C. & Georgiou, G. Serology in the 21st  
403 century: the molecular-level analysis of the serum antibody repertoire. *Curr. Opin.*  
404 *Immunol.* **35**, 89–97 (2015).
- 405 30. Perlot, T., Alt, F. W., Bassing, C. H., Suh, H. & Pinaud, E. Elucidation of IgH  
406 intronic enhancer functions via germ-line deletion. *Proc. Natl. Acad. Sci.* **102**,  
407 14362–14367 (2005).
- 408 31. Laserson, U. *et al.* High-resolution antibody dynamics of vaccine-induced immune  
409 responses. *Proc. Natl. Acad. Sci. U. S. A.* **111**, 4928–33 (2014).
- 410 32. Glanville, J. *et al.* Precise determination of the diversity of a combinatorial  
411 antibody library gives insight into the human immunoglobulin repertoire. *Proc.*  
412 *Natl. Acad. Sci. U. S. A.* **106**, 20216–21 (2009).
- 413 33. Wang, C. *et al.* B-cell repertoire responses to varicella-zoster vaccination in  
414 human identical twins. *Proc. Natl. Acad. Sci. U. S. A.* **112**, 500–5 (2015).
- 415 34. Tipton, C. M. *et al.* Diversity, cellular origin and autoreactivity of antibody-  
416 secreting cell population expansions in acute systemic lupus erythematosus. *Nat.*  
417 *Immunol.* **16**, 755–65 (2015).
- 418 35. Li, W. & Godzik, A. Cd-hit: a fast program for clustering and comparing large sets  
419 of protein or nucleotide sequences. *Bioinformatics* **22**, 1658–9 (2006).
- 420 36. Krzywinski, M. *et al.* Circos: an information aesthetic for comparative genomics.  
421 *Genome Res.* **19**, 1639–45 (2009).
- 422
- 423

424 **FIGURE LEGENDS**

425

426 **Figure 1. Serial sampling, isolation by FACS, and NGS of BM PCs reveal temporal**  
427 **dynamics of antibody repertoire.** (a) Overview of antibody repertoire characterization  
428 method. Serial sampling of human bone marrow plasma cells (BM PCs) over 6.5 years  
429 (left). Analysis of individual genes, gene combinations, and CDR-H3s (center) show  
430 temporally stable expression of persistent entities (right). (b) Representative  
431 fluorescence-activated cell sorting (FACS) gates of BM PCs (CD138+, CD38++) isolated  
432 from bone marrow mononuclear cells (BMMCs). (c) Sample collection timeline and  
433 summary of cell counts, sequencing reads, and unique CDR-H3s.

434

435 **Figure 2. Individual gene use frequencies for Donor 1 are temporally stable.** (a-c)  
436 IGHV (a), IGHD (b), and IGHJ (c) gene usage frequency over time. Plots are sorted by  
437 decreasing mean frequency. Only gene calls that appear in all timepoints are shown. (d)  
438 Mean frequency of IGHV gene use. Error bars are standard deviation.

439

440 **Figure 3. Usage frequencies of gene combinations are temporally stable.** IGH V-J  
441 usage frequencies for Donor 1 are shown. Plots are sorted by decreasing mean  
442 frequency. Only gene calls that appear in all timepoints are shown. See Supplementary  
443 Figure 1(a-c) for usage frequencies of IGH V-D, D-J, and V-D-J.

444

445 **Figure 3. Gene combinations do not preferentially associate and are instead**  
446 **randomly assorted.** (a-d) Spearman's rank correlation of expected versus observed  
447 IGH V-D (a), V-J (b), D-J (c), and V-D-J (d) gene combination frequencies. Expected (by  
448 random association) frequencies are calculated as products of the frequencies of the  
449 individual component genes. Diagonal lines in red indicate no difference between the  
450 expected and observed frequencies.

451

452 **Figure 5. Usage frequencies of persistent clonotypes are temporally stable.** (a)  
453 Circos plot of shared clonotypes between adjacent timepoints (top). Circos plot of the  
454 persistent clonotypes across all timepoints (bottom). Each band in the outermost  
455 perimeter represents the clonotypes found in a given timepoint, sorted by decreasing  
456 expression. The inner curved lines indicate the same clonotype shared by two  
457 timepoints. Green indicates high expression; purple, low expression; with lighter colors

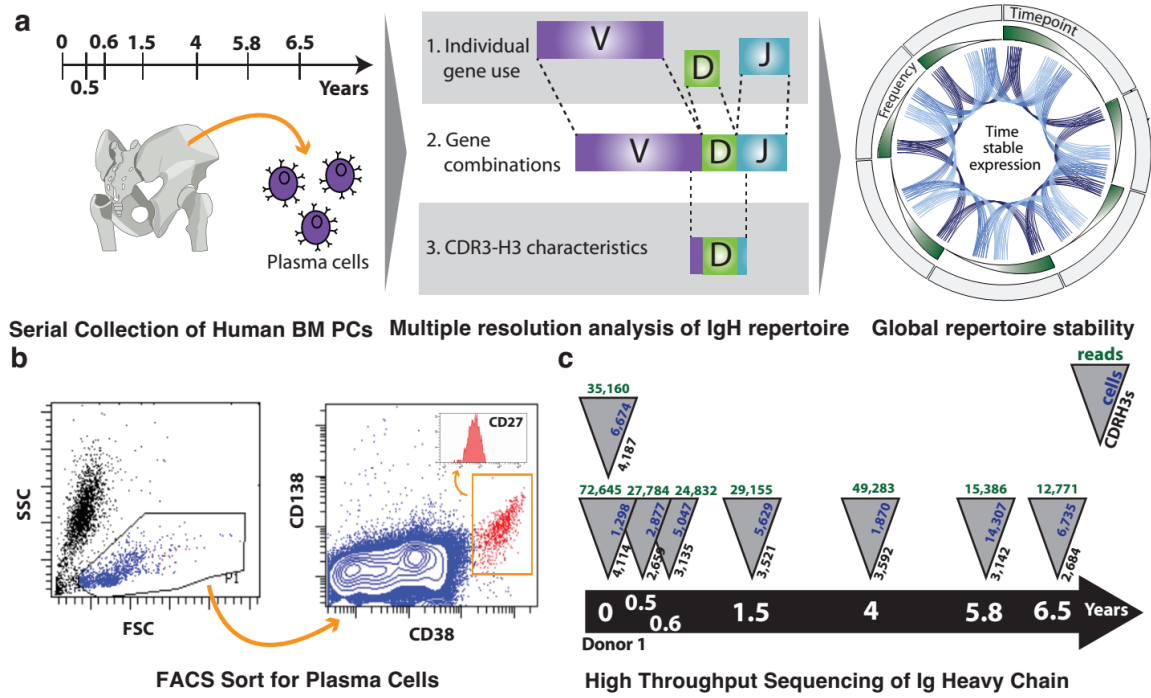
458 indicating intermediate expression. (b) Gene usage frequency over time of the 23  
459 persistent clonotypes (see Methods) found in all timepoints. Plots are sorted by  
460 decreasing mean frequency. Gene names (for IGHV and IGHJ), representative amino  
461 acid sequences, and isotype are above each plot.

462

463 **Figure 6. Gene and gene combination use frequencies correlate between Donor 1**  
464 **and Donor 2.** (a) Spearman's rank correlation of individual gene frequencies between  
465 the two donors: IGHV (top), IGHD (center), and IGHJ (bottom). (b-e) Spearman's rank  
466 correlation of combination gene frequencies between the two donors: V-D (b), V-J (c), D-  
467 J (d), and V-D-J (e). (a-e) Red lines indicate least squares regression.

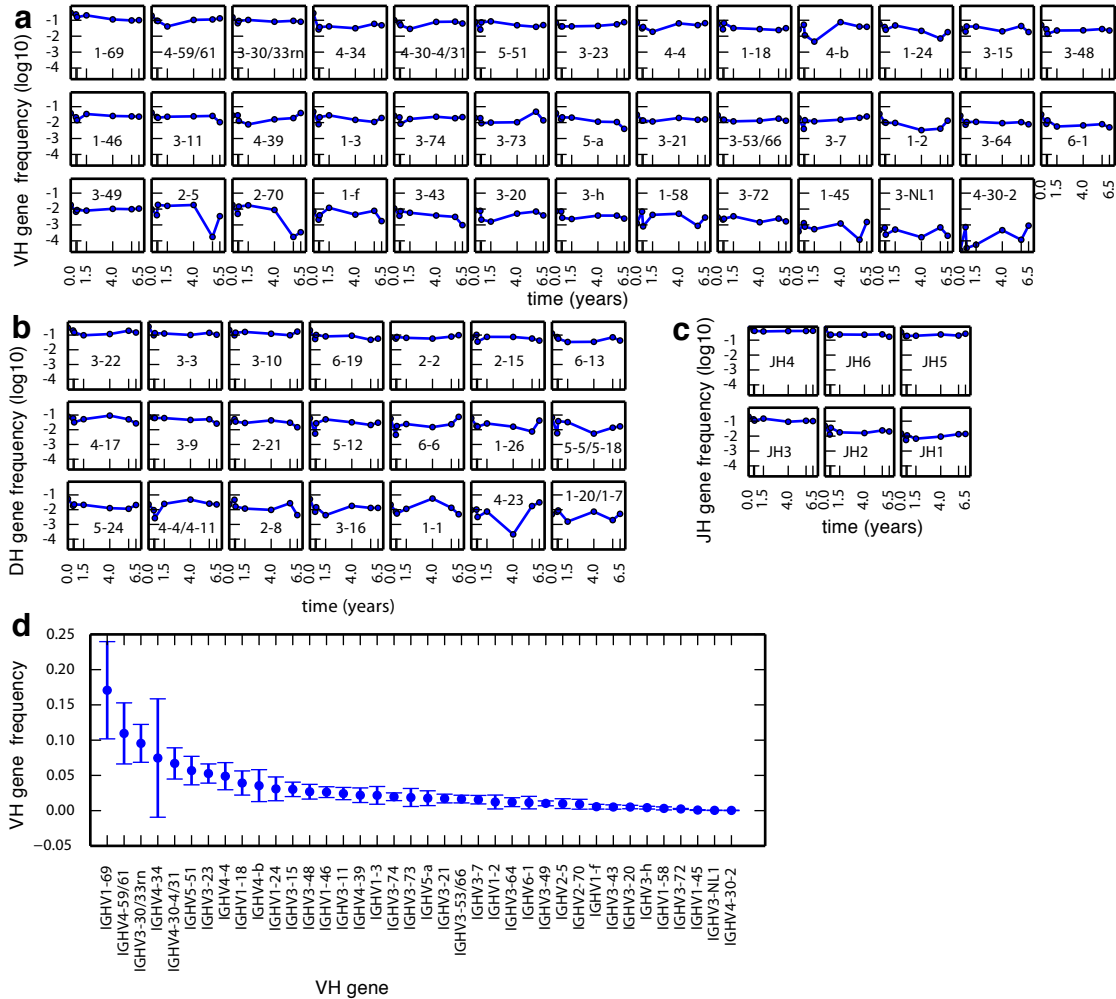
468





469  
470  
471  
472  
473  
474  
475  
476  
477  
478  
479  
480  
481  
482  
483  
484  
485  
486  
487  
488  
489  
490  
491

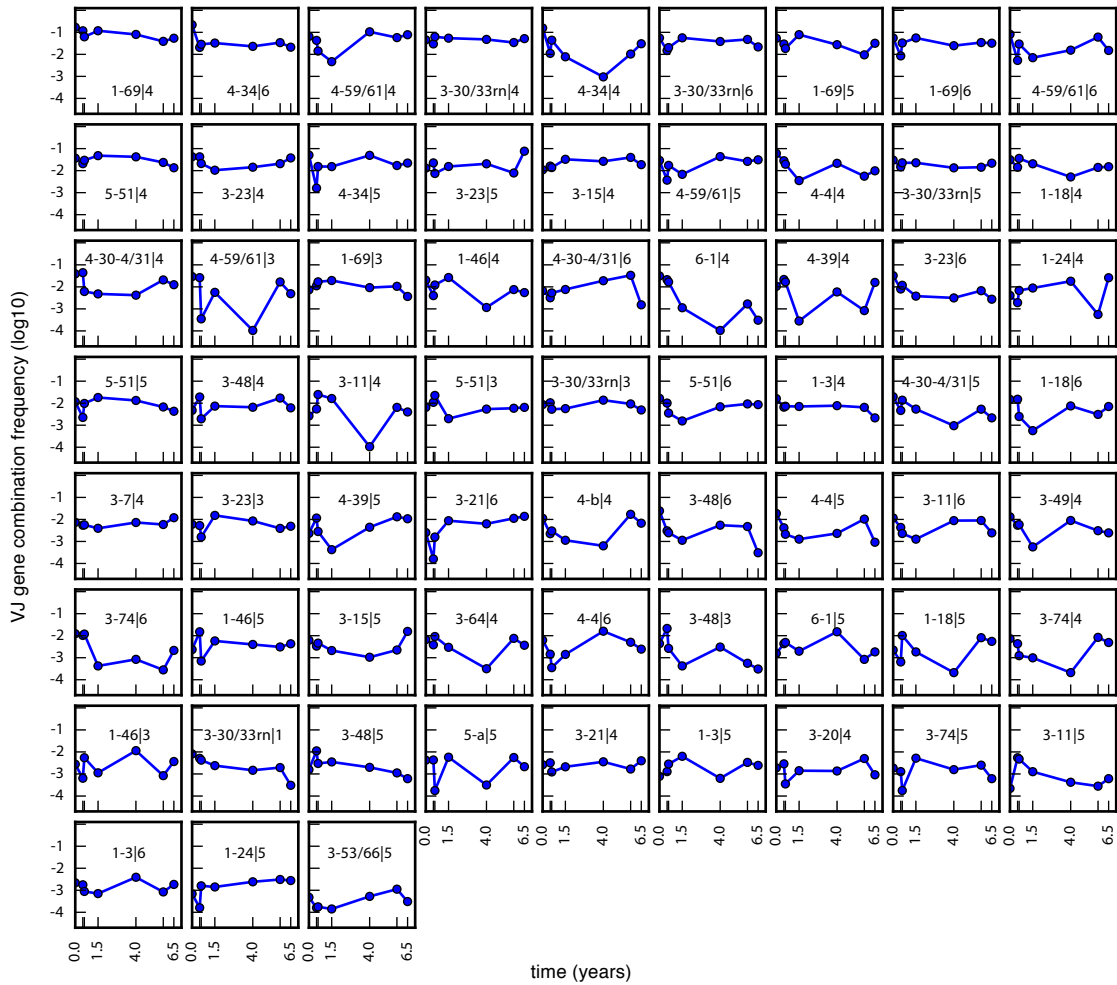
**Figure 1**



492  
493  
494  
495  
496  
497  
498  
499  
500  
501  
502  
503  
504  
505  
506  
507  
508  
509  
510  
511  
512  
513

Figure 2

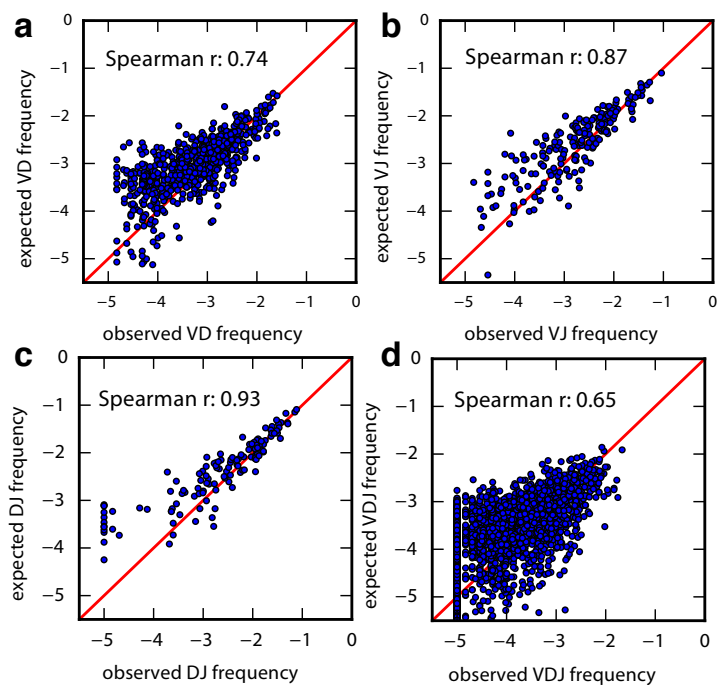
514  
515  
516  
517  
518



519  
520  
521  
522  
523  
524  
525  
526  
527  
528  
529  
530  
531  
532

**Figure 3**

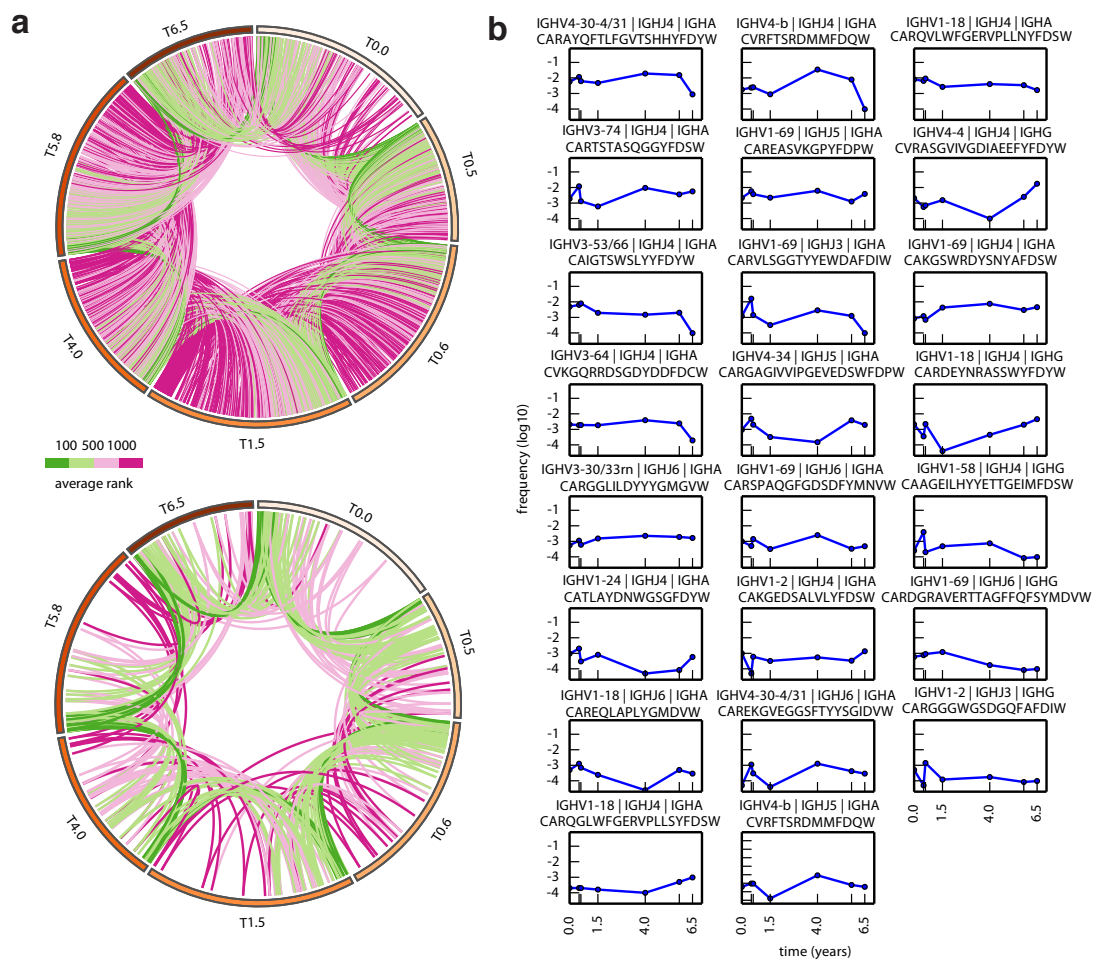
533  
534  
535  
536  
537  
538  
539



540  
541  
542  
543  
544  
545  
546  
547  
548  
549  
550  
551  
552  
553  
554  
555  
556  
557  
558  
559  
560

**Figure 4**

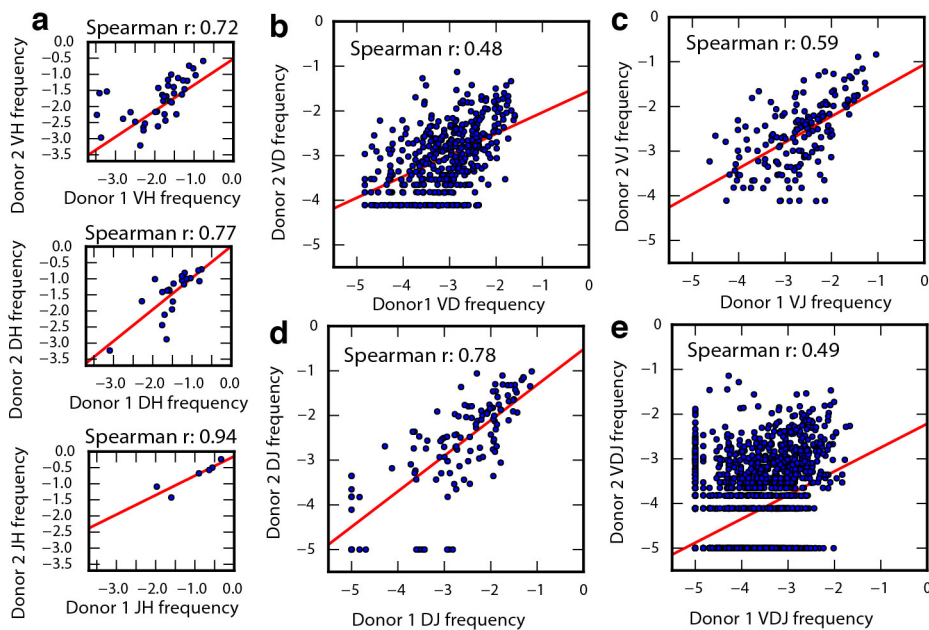
561  
562  
563  
564  
565



566  
567  
568  
569  
570  
571  
572  
573  
574  
575  
576  
577

**Figure 5**

578  
579  
580  
581  
582



583  
584  
585  
586  
587  
588  
589  
590  
591  
592  
593  
594  
595  
596  
597  
598  
599  
600  
601  
602  
603

Figure 6